

LOW-TEMPERATURE AG-PASTE SCREENING FOR SILICON HETEROJUNCTION SOLAR CELLS AND MODULES

S. Pingel¹, D. Erath¹, T. Wenzel¹, S. Nold¹, D. Eberlein¹, A. De Rose¹, S. Tepner¹, J. Schube¹, G. Ivanov², E. Terukova²
A. Moldovan¹, A. Lorenz¹ and F. Clement¹

¹Fraunhofer Institute for Solar Energy Systems ISE

Heidenhofstrasse 2, 79110 Freiburg, Germany

Phone +49 761/4588-2180

sebastian.pingel@ise.fraunhofer.de

²R&D Center TFTE

Polytechnicheskaya 28, 194021 Sankt-Petersburg, Russia

ABSTRACT: This paper addresses the testing of eleven different low-temperature pastes (LTP) for silicon heterojunction (SHJ) solar cells. In the LTP screening different pastes from different suppliers were printed on the front side of industrial rear-emitter transparent conductive oxide TCO precursors with industry relevant screens. The pastes are compared with regard to (1) electrical properties of the grid fingers for screen openings ranging from 50 μm over 40 μm down to 30 μm and (2) the suitability for module integration which is addressed by peel tests after the soldering step and (3) performance on cell level for busbarless (OBB) and five busbar (5BB) technology as well as (4) economic factors like laydown and fast printing compatibility which affects through-put of screen printing in the production line.

Keywords: Heterojunction, Metallization, Screen Printing, Module Integration

1 INTRODUCTION

Silicon heterojunction (SHJ) technology is one of the next generation high efficiency concepts that are currently in the focus of the PV community enabling record solar cell efficiencies [1,2] and increasing in market share [3,4]. One drawback of the SHJ technology is that the metallization needs to be adapted since the a-Si:H surface passivation layers and transparent conductive oxide (TCO) are temperature sensitive and firing contact technology cannot be applied without degrading the passivation. At Fraunhofer ISE different metallization technologies for SHJ cells are investigated [5-7]. The technology typically applied in industrial mass production to form the contacts on SHJ cells is low-temperature paste (LTP) based on silver particles that are screen printed, dried and cured. Here temperature for contact formation can be reduced to around 200°C. Compared to firing Ag-pastes the LTPs suffer from increased line and contact resistance due to paste composition and high porosity of the grid finger after curing. In industry this leads to comparatively wide fingers (about 50 μm) and high silver paste consumption. The major targets for the LTP and contact formation process development are to reduce costs, increase efficiency and enable flexible module integration with long-term reliable interconnection. The targets for paste development split in the following topics: (1) electrical properties of the grid fingers for screen openings ranging from 50 μm over 40 μm down to 30 μm and (2) the suitability for module integration which is addressed by peel tests after the soldering step and (3) performance on cell level for busbarless (OBB) and five busbar (5BB) technology as well as (4) economic factors like paste laydown, fast printing and curing compatibility which both affect through-put of metallization process in the production line.

2 AIM AND APPROACH

To address the targets for SHJ low-temperature metallization mentioned in the introduction eleven different LTPs based on silver (Ag) are compared for suitability in a SHJ cell and module process, see Fig. 1.

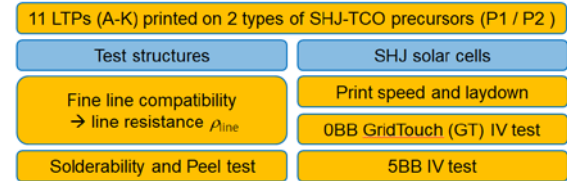


Figure 1: Overview of investigated topics in the experiment.

In the first step all eleven pastes are printed as test structures on two types of industrial TCO precursors (P1 and P2) to test fine line compatibility as well as suitability for module integration which is addressed by peel tests after a conventional soldering step with an industrial IR stringer. Secondly OBB cells are printed, again with all eleven pastes and on the two types of precursors, cured and measured with a Grid Touch unit (GT). Finally these are converted by an extra printing step of busbars to 5BB cells and measured again after a second curing. As economic factors of the front side print step (i) paste compatibility with increased print speed of 200 mm/s is tested and (ii) paste consumption is recorded.

2 RESULTS

2.1 Test structures

The suitability of the LTPs for different screen openings was investigated by printing test structures with varying screen opening ($w_n = 30, 40$ and $50 \mu\text{m}$). The line resistance ρ_{line} was measured after a 10 min curing step at 200°C curing. The ρ_{line} data is shown in Fig. 2 and the range of ρ_{line} for the different openings is summarized in table I.

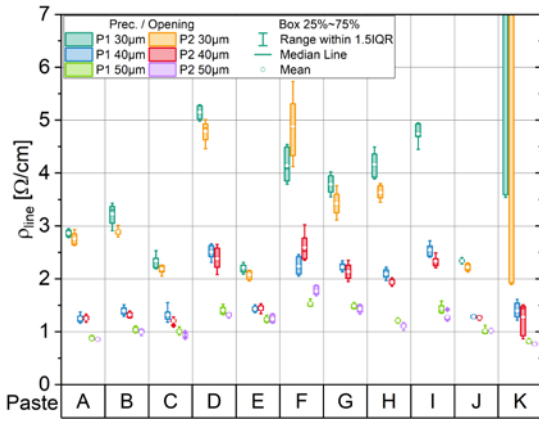


Figure 2: Line resistance ρ_{line} for the different LTPs and screen openings of w_n 30, 40 and 50 μm

Table I: Range of line resistance ρ_{line} and the relative spread for different pastes and screen openings w_n .

Opening w_n	ρ_{line} range [Ω/cm]	relative spread ρ_{line} (max-min)/median
30 μm	2.1 - 12.0	280%
40 μm	1.2 - 2.5	90%
50 μm	0.8 - 1.7	80%

The ρ_{line} is on a similar level for precursor type P1 and P2, but overall a slightly lower ρ_{line} was found for P2. This can be explained by the higher paste laydown on this type of precursor. The reason for this is not yet investigated but differences in texture or the TCO properties might explain the deviation. All pastes are in principle suitable for w_n of 40 and 50 μm , but the ρ_{line} varies significantly for the different types of paste. For narrower opening with a w_n of 30 μm variability increases drastically, only half of the pastes show $\rho_{line} < 4 \Omega/cm$.

To estimate the front side contribution of ρ_{line} to the series resistance (R_s) the *GridRES* is calculated for a fixed number of grid fingers ($n_{finger} = 80$) for different busbars configurations (n_{BB}) by the following formula:

$$GridRES_{FS} = \frac{\rho_{line} \cdot l_{cell}^3}{12 \cdot n_{finger} \cdot n_{BB}^2}$$

Here l_{cell} is the edge length of the wafer (M2: 156.75 mm). The resulting data is shown in Fig. 3 below.

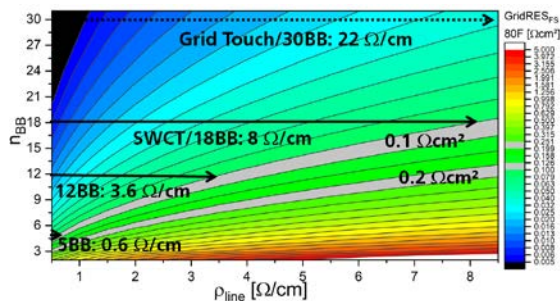


Figure 3: Front side grid resistance contribution to R_s as a function of ρ_{line} and the number of busbars for a 80 finger grid. For certain BB configurations the necessary ρ_{line} is indicated to reach a *GridRES* of $0.1 \Omega/cm^2$

For a large number of busbars or wires (e.g. in the IV measurement with a GT unit 30 current wires are contacting the grid) *GridRES* is rather low and the effect

on the total cell series resistance R_s is negligible. For lower n_{BB} the impact of ρ_{line} increases. The necessity to reach a *GridRES* of $0.1 \Omega/cm^2$ is indicated in Fig. 3 for certain BB configurations. An additional R_s of $0.1 \Omega/cm^2$ causes a fill factor (*FF*) loss of about 0.5%. For 80 fingers and 5BB a $\rho_{line} < 0.6 \Omega/cm$ is needed to keep *GridRES* below this level, none of the tested pastes and screen opening combinations reached this target. An option would be to increase the number of grid fingers or increase the screen opening w_n . Both options would increase the paste laydown. For measurements with the GT unit all tested paste and opening combinations reached the target ($\rho_{line} < 22 \Omega/cm$). This leads to the conclusion that for 0BB IV cells the paste selection is relaxed in terms of ρ_{line} , but for 5BB the paste selection is quite limited for high efficiency SHJ solar cells with a low number of fingers, as will be shown in section 2.3.

2.2 Solderability for module integration

At last year's EUPVSEC it was shown that SHJ cells can be interconnected with a conventional industrial IR stringer [8]. But one of the issues after the SHJ cell interconnection is the rather low adhesion of the LTP to the TCO after curing and subsequently soldering ribbons on the BBs. To investigate the suitability of the pastes for conventional module integration 0.8 mm wide continuous busbars were printed on the two types of precursors. After a 10 min 200°C curing step soldering was done on an industrial IR stringer with a PV ribbon (Cu core 0.9x0.22 mm², Sn60Pb40 coating). Adhesion was tested by a peel test (FS & RS under 90°) that yielded the normalized peel force: F/w , where F is the recorded peel force and w is the width of the BB. The results are shown in Fig. 4. Most of the pastes showed rather poor adhesion with $F/w < 0.3$ N/mm or the pastes could not be soldered at all (missing data points). Only two pastes "D" and "I" achieved with 1.1 to 1.5 N/mm and 0.8 to 1.0 N/mm respectively significant adhesion. The effect of F/w on long term reliability will be tested in the near future.

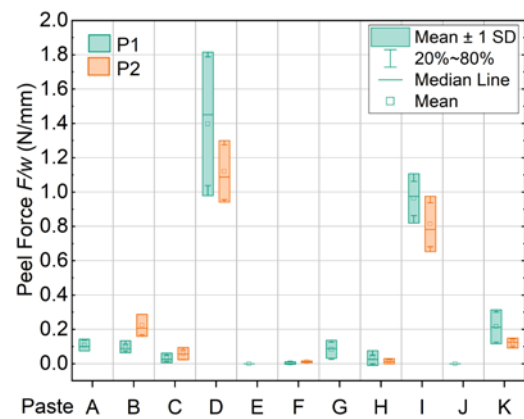


Figure 4: Normalized peel force for the eleven LTPs on P1 / P2. For the missing groups: no soldering was possible

2.3 Solar cells

To investigate the effect of LTP type on cell level SHJ solar cells were produced on SHJ precursors (20 per type P1 and P2, total 40). First the rear side (RS) grid

(150F/50 μm) was printed with a reference paste on the two types of industrial precursors. After drying the front side (FS) grid (80F/40 μm) was printed and again dried. After a short curing step of 5 min at 200°C the finished OBB cells were IV measured with a GT unit. After measurement the cells were converted to 5BB by printing the BBs on RS and FS (dual printing). After another short curing step the 5BB cells were measured on the IV tester. The process is shown in Fig. 5 below.

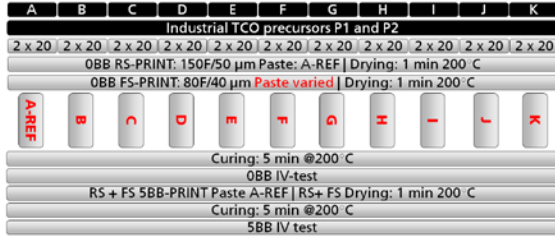


Figure 5: Process sequence for OBB/5BB solar cells based on industrial SHJ precursors.

As expected the efficiency is decreased for 5BB due to additional shading by the BBs and the larger spacing between the current contacts (5.2 mm for OBB vs 31.2 mm for 5BB). Typically the found efficiency (η) drop was about 0.6%, with a minimum drop of 0.3% and a maximum drop of 1.0% for the different pastes. The results are summarized in Table II.

Table II: Median efficiencies for all paste groups for OBB and 5BB configuration on the two industrial precursors.

Pre-cursor	Med. η -OBB	Range	Med. η -5BB	Range
P1*	21.9%	$\pm 0.1\%$	21.3%	$+0.3/-0.4\%$
P2	22.7%	$\pm 0.1\%$	22.1%	$\pm 0.3\%$

*: For P1 and OBB one outlier group was excluded due to unexpected low efficiency that is unlikely caused only by the paste.

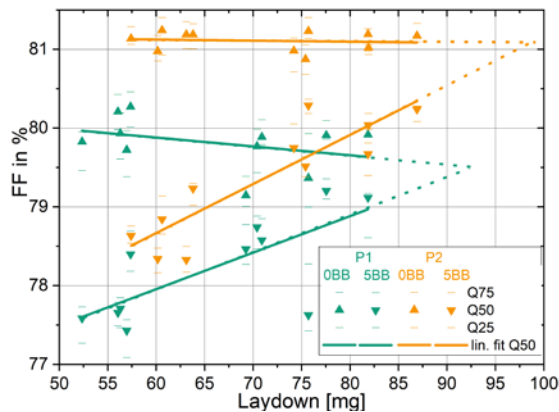


Figure 6: Fill factor as a function of FS median paste laydown (different pastes printed with the same screen opening) for two precursor types P1 and P2.

Fig. 6 above shows the impact of the paste type and laydown using a 40 μm screen opening on the FF. For OBB no FF increase is detected for pastes that were printed with high laydown compared to pastes with low

laydown. This is valid for both types of precursors. This is indicated by linear fits that show no slope for OBB for P2 and an even slight negative trend for P1. For 5BB increased laydown leads to higher FF, visible in the line fits with positive slope for both precursor types. This result is in good agreement to the results found for the fine line test structures with the same w_n of 40 μm (Fig. 2) and the simulation of the impact of the number of BB (Fig. 3). According to the linear trends similar FF for OBB and 5BB are expected for paste laydown in the range of 90-100 mg. This would lead to quite high paste consumption to achieve high FF values for 5BB cells. The cost optimum is expected to be found at lower laydowns. Future work will address optimal finger width, pitch and paste laydown for SHJ cells with busbars.

3 ECONOMICAL APECTS

The processes for metallization are contributing significantly to the total costs of SHJ solar cells. Especially paste consumption and price are important [7,9]. As described in the introduction metallization of SHJ cells is more challenging. Commercially available LTPs are typically not yet printable at high speeds which are currently used in PERC production (600 mm/s). Within this investigation the LTPs were tested for compatibility with increased print speed of 200 mm/s, two pastes could be printed with only about 100 mm/s, while nine out of eleven LTPs could be printed with 200 mm/s. This is close to the speed relevant for industrial SHJ production. Fig. 7 shows the impact of the print and flood speed on the normalized CAPEX (capital expenditure) of the screen printing process. Doubling the speed from 200 to 400 mm/s reduces the CAPEX by about 40%. Higher speeds will be tested in the future to further reducing the costs for SHJ metallization in production.

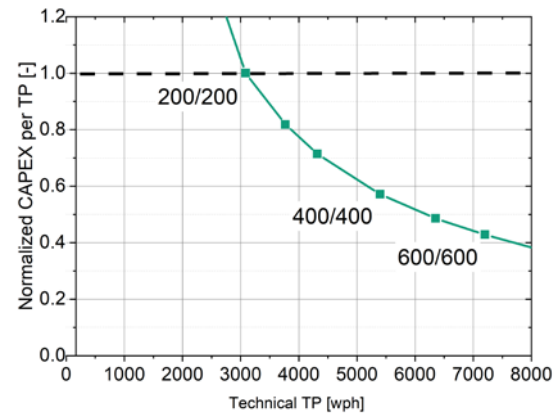


Figure 7: Normalized CAPEX for screen printing as a function of technical wafer throughput put that is linked to the print and flood speed for a dual print line.

The utilization of LTP leads to another disadvantage for SHJ, low-temperature processing and paste composition results in higher line resistance. This can be addressed by increasing the paste laydown, a quite expensive option. An alternative is to decrease the finger length between the current contacts (e.g. smart wire interconnection or multi busbar technology: SWCT or MBB [10,11]). In this paste screening the FS grid finger paste consumption varies in the range 70 ± 20 mg (almost $\pm 30\%$) for the

same screen opening and grid layout. Comparing the two types of precursors it was found that P2 showed a 4% increased laydown compared to P1 in average for all pastes, see also section 2.1. This means that processes prior to screen printing have an impact on the paste consumption.

For busbarless cells a comparatively low laydown is sufficient to achieve high efficiency in the IV test with the GT unit. The technology has quite substantial cost saving potential. But in the module typically less than 30 ribbons or wires are applied for interconnection, correspondingly the impact of the line resistance increases to some extent, see Fig. 3. For 5BB cells high laydown yielded higher efficiency. For a certain price for the LTP the optimum can be derived but is not part of this investigation. To reduce the paste consumption the ρ_{line} needs to be improved (paste, printing and curing optimization) or the busbar configuration needs to be adapted, meaning a higher number of BB / ribbons or wires for interconnection.

4 SUMMARY AND OUTLOOK

In this test eleven different LTPs were compared in terms of fine line suitability. For all pastes printing with a screen opening w_n of 40 μm and 50 μm reasonable ρ_{line} and print quality was found, while going down to w_n of 30 μm lead to a strong variation in ρ_{line} . For a high number of BB this lead to negligible FF-losses but for mainstream 5 or 6 BB the paste needs to be carefully selected when printing fingers with narrow openings. For module integration by conventional soldering suitable LTPs could be identified, most of the pastes show poor adhesion that will likely lead to problems during handling of the cell strings in production as well as in the long-term reliability testing. But two pastes showed increased adhesion. The effect on module reliability of the peel force of the soldered ribbon on LTP will be studied in future investigations.

In a second test the FS grid of cells were printed with the different LTPs. For 0BB measurement a rather small influence of the paste was found. After conversion to 5BB the variability increased significantly due to different pastes, their laydown and the resulting ρ_{line} . The cell results are in good agreement with the ρ_{line} measurements on test structures. The highest 5BB η was found for pastes with high laydown. Due to the high silver content of the paste the laydown has a strong impact on the costs per cell. The target for the future is more efficient paste utilization. Here advanced screens with adapted mesh and coatings [12-14] are an interesting option. These screens allow potentially more uniform fingers with reduced paste consumption. For high temperature paste finger widths below 20 μm were already realized [15,16] but also for LTP [17]. Another economical factor is the print speed. With increasing speed screen printer utilization is improved subsequently the CAPEX is reduced. Most of the pastes allow printing with 200 mm/s. In the future higher print speed and the effect of reduced w_n will be studied.

5 REFERENCES

- [1] Adachi et al.: "Impact of carrier recombination on fill factor for large area heterojunction crystalline silicon solar cell with 25.1% efficiency", APL 2015
- [2] Yoshikawa et al.: "Silicon heterojunction solar cell with interdigitated back contacts for a photoconversion efficiency over 26%", Nature Energy 2017
- [3] ITRPV: "International Technology Roadmap for Photovoltaic (ITRPV)", 10th edition 2019
- [4] Taiyang News: "Heterojunction Solar Technology 2019 Edition"
- [5] D. Erath et al.: "Comparison of innovative metallization approaches for silicon heterojunction solar cells", Silicon PV 2017
- [6] J. Schube et al.: "Low-Resistivity Screen-Printed Contacts on Indium Tin Oxide Layers for Silicon Solar Cells With Passivating Contacts", IEEE 2018
- [7] T. Hatt et al.: "Low-cost Cu-plated metallization on TCOs for SHJ Solar Cells – Optimization of PVD Contacting-layer", IEEE 2020
- [8] A. De Rose et al.: „Interconnection of silicon heterojunction solar cells by infrared soldering – solder joint analysis and temperature study“, EU PVSEC 2019
- [9] S. Nold: "Techno-ökonomische Bewertung neuer Produktionstechnologien entlang der Photovoltaik-Wertschöpfungskette" PhD University Freiburg 2019
- [10] A. Faes et al.: "Smartwire solar cell interconnection technology", EU PVSEC 2014
- [11] S. Braun et al.: "Multi-busbar solar cells and modules: high efficiencies and low silver consumption", Silicon PV 2013
- [12] S. Tepner et al.: "Screen Pattern Simulation for an Improved Front-Side Ag-Electrode Metallization of Si-Solar Cells", Prog. Photovolt: Res. Appl. (2020)
- [13] S. Tepner et al.: "Improving Wall Slip Behavior of Silver Pastes on Screen Emulsions for Fine Line Screen Printing", Solar Energy Materials and Solar Cells 200 (2019) 109969.
<https://doi.org/10.1016/j.solmat.2019.109969>
- [14] S. Tepner et al.: "Studying Knotless Screen Patterns for Fine Line Screen Printing of Si-Solar Cells", IEEE J. Photovoltaics (2020).
<https://doi.org/10.1109/JPHOTOV.2019.2959939>
- [15] F. Clement et al.: "Project Finale – Screen and screen printing process development for ultra-fine contacts below 20 μm finger width", EU PVSEC 2019
- [16] S. Tepner et al.: "Advances in Screen Printed Metallization for Si-Solar Cells -Towards Ultra-Fine Line Contact Fingers Below 20 μm ", Asia PVSEC 2019
- [17] A. Descoeudres et al.: "Low-temperature processes for passivation and metallization of high efficiency crystalline silicon solar cells" Solar Energy 2018